International Journal of Development Mathematics Vol 1 Issue 2, Page No. 061 - 080

INTERNATIONAL JOURNAL OF DEVELOPMENT MATHEMATICS

ISSN: 3026-8656 (Print) | 3026-8699 (Online)

journal homepage: https://ijdm.org.ng/index.php/Journals

Mathematical Assessment of Covid-19 Transmission Dynamic with Intervention via: ABC Fractional Operator

Ayuba Sanda[a,b^], Oladejo O. Semiu[a,b], Albert A. Shalangwa[a,b], Yahaya Ajiya[a,b] and Ishiaku Zubairu[a,b]

[a]*Department of Mathematical Sciences, Faculty of Science, Gombe State University, Gombe, Nigeria.*

[b]*GSU-Mathematics for Innovative Research (GSU-MIR) Group, Department of Mathematical Sciences, Gombe State University, Gombe, Nigeria.*

ARTICLE INFO

Article history:
Received 15 March 2024
Received in revised form 06 June 2024
Accepted 18 June 2024

Keywords:
ABC-Operator, Covid-19, Intervention, Stability Analysis

MSC 2020 Subject classification:
62M08, 62M10, 62P10, 62F01

ABSTRACT

A Covid-19 model in terms of the ABC operator with intervention is developed and used to study the disease transmission dynamics. The model showed stability when the basic reproduction number is less than unity, indicating that each existing infection causes less than one new infection, resulting in a decline in cases. A stable system and a basic reproduction number ($\mathcal{R}_0$) value greater than unity suggest exponential growth of the disease. The model was fitted using NCDC data from March 4 to April 30; 2022 and the sensitivity analysis reveals effective contact rates and transmissibility of asymptomatic individuals as the most sensitive parameters. Numerical simulations reveal that increased effective contact rate (social distancing) increases virus spread, while increased face mask compliance reduces exposure and infection rates. Hence wearing face masks reduces respiratory droplet transmission, reducing the need for quarantine and reducing infection rates.

1. Introduction

The transmission dynamics of COVID-19, caused by SARS-CoV-2, has been a subject of extensive research, crucial for effective control measures and public health strategies. The Sars-CoV-2 coronavirus, first detected in Wuhan, China, has since infected over 560 million people and caused six million fatalities. The World Health Organization declared a pandemic in March 2020, prompting the scientific community to combat COVID-19, (WHO, 2020; Jia *et al.,* 2020; Prem *et al.,* 2020; Worldometers, 2021). Mathematical modeling is crucial for understanding disease spread. Research focuses on effective treatments, vaccines, and forecasting infection trends using mathematical and statistical modeling (Alam *et al.,* 2022; Xu and Tang, 2021; Nguyen *et al.,* (2021). Ferguson *et al,* (2020) studied a significant early contribution in this field, gained international recognition for its insightful insights. Researchers used the SIR model to construct deterministic structures using differential equations (Brauer, 2005; Cortés-Carvajal, Cubilla-Montilla and González-Cortés, 2022). Peng (2022) proposed a generalized SEIR model for COVID-19, incorporating self-protection and quarantine compartments. Jia (2020) suggested an adjusted model for quarantined populations. Castilho (2020) presented a generalized version for age-structured populations. Nigeria recorded its first COVID-19 case in February 2020, with the highest number of confirmed cases of 55,005 and 1,057 deaths. In January 2021, the number rose to 142,579 cases, with 1,702 casualties and 118 thousand recoveries. Nigeria is the sixth top-ranked African country in reported cases, with the highest daily increase since the pandemic began. Mathematical models have proven reliable tools for implementing control measures to prevent and minimize infectious disease impact, (Madubueze *et al.,* 2018; Kim 2016). Sun *et al,* (2023), studied the instances of coronavirus infection from Pakistan to estimate parameters and provide solutions for disease elimination. It investigated a fractional order model of vaccine efficacy and fading immunity in coronavirus infection. Ega and Ngeleja (2022) mathematical model revealed COVID-19 transmission is influenced by both symptomatic and asymptomatic cases, suggesting measures to remove the virus and lower infection rates may reduce secondary infections. Moderate social-distancing tactics, such as face masks, can effectively suppress COVID-19 in Nigeria, according to a mathematical model by Iboi *et al,* (2020), advocating community lockdown measures for at least three to four months. Abioye *et al,* (2021), presented a mathematical model for COVID-19, recommending effective management in Nigeria through face-mask use, social distancing, patient treatment, and prevention. They find that reducing the fractional operator lowers the number of infections. The fractional calculus model enhances understanding of population interactions; enabling accurate disease

* Corresponding author. Tel.: +23465874739
E-mail address: *ayubasanda@gsu.edu.ng* (Ayuba S.)
https://doi.org/10.62054/ijdm/0102.05

spread predictions and evaluation of control strategies like social distancing and quarantine protocols, providing valuable insights for policymakers and healthcare professionals. Baba *et al,* (2022) developed a COVID-19 Awareness model using fixed point theorems, predicts-corrector approach, and graphs with varying parameter values. In their study, Okyere *et al*, (2023) evaluated Tuberculosis-COVID-19 co-infection using fractional-order derivative modeling. In their study on coronavirus infection, Sun *et al*, (2023) emphasized the significance of vaccination in illness control by examining vaccine efficacy and decreasing immunity using a fractional order model. Sinan and Alharthi (2023) used a dynamical system with a fractal-fractional-order derivative to investigate the psychological consequences of COVID-19. They found both global and local stability and used Pontryagin's maximum principle and bifurcation analysis to anticipate the spread of the disease. Ahmed *et al,* (2020) mathematical model utilized five nonlinear fractional-order differential equations and the fractional Euler method to analyze lock-down effectiveness in mitigating coronavirus spread. A Bats-Hosts-Reservoir-People transmission model was examined and examined by Shaikh *et al.* (2020) in order to replicate fractional-order COVID-19 transmission and individual response. The model forecasts future outbreaks, evaluates the efficacy of preventive measures, and makes recommendations for control tactics. In order to replicate the transmission of COVID-19, Adel *et al.* (2024) divided the population into four categories: susceptible, infected, treated, and recovered. They emphasized the need for restraints by using numerical simulations and Laplace Adomian decomposition. For the purpose of analyzing virus dynamics, Saleem *et al*. (2024) created the fractional order epidemic model (SIVR). By employing stability analysis and standard results, the model guarantees positivity and boundedness. Control measures, according to simulations, boost recovered populations while decreasing infected ones. One helpful tool for simulating COVID-19 dynamics is the ABC fractional operator. It allows for more precise forecasts by capturing intricate, non-local, and memory-dependent patterns in the transmission of infectious diseases. In order to better understand the effects of interventions, the persistence of outbreaks, and the effectiveness of control measures, long-range dependency is also taken into account. Because the operator is flexible, scientists can incorporate other factors into the model. As a result, forecasting disease transmission and the effectiveness of control measures is achievable with greater accuracy. It also gives policymakers more predictive ability, enabling them to anticipate potential outbreaks, deploy resources effectively, and implement treatments on time. Furthermore, the ABC fractional operator advances epidemiological knowledge by making it easier to identify critical factors influencing transmission and by promoting the use of evidence in decision-making (Vasily, 2021). It can generally guide policy decisions, guide public health initiatives, and mitigate the pandemic's effects. Inspired by the above literature review; we extended and modified the Abioye *et al,* (2021) model to develop a fractional COVID-19 model by adding interventions such face mask use, quarantine, and memory effect and utilizing a fractional derivative of the Atangana Bealenu operator.

2. Model Formulation

The total population of the modified model of COVID-19 at time (t) is denoted by $N(t)$ and is divided in to six (6) compartments. Viz: The susceptible population $S(t)$ represents individuals who have not been infected but are at risk of contracting the virus. The exposed population $E(t)$ consists of individuals who have been exposed to the virus but are not yet infectious. Asymptomatic individuals $A(t)$ are carriers of the virus who do not show symptoms but can still transmit the disease. Symptomatic individuals $I(t)$ show signs of the disease and are typically the most infectious group. Quarantined individuals $Q(t)$ are those who have been isolated to prevent further spread of the virus. Finally, the recovered population $R(t)$ includes individuals who have either survived the disease and developed immunity or succumbed to it. Λ is the human recruitment rate into the susceptible class, the susceptible individuals becomes exposed when coming in contact with either asymptomatic or symptomatic infected individual at a rate β_a and β_s respectively, while $0 \le l \le 1$, measure the population's transmissibility without symptoms. $0 < a \le 1$ and $0 < e \le 1$, are the percentage of people who wear masks and the effectiveness of face masks. η is the progression rate to the symptomatic class ($1/\eta$ is the average incubation time of covid-19) and θ, is the fraction of the exposed individual with clinical sign, while $(1-\theta)$ shows no clinical symptom and progress to the A. υ and ε are recovery rate, while ρ and τ are quarantine rate for asymptomatic and symptomatic respectively. ω, is the recovery rate for the quarantine class.

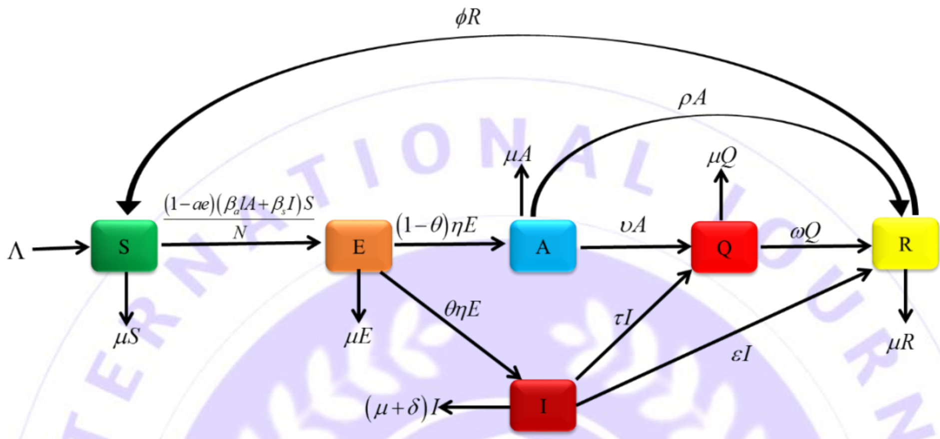

Figure 1: Diagram providing the system's summary of the COVID-19 model (1)

$$\left.\begin{aligned}
{}_{0}^{ABC}D_t^{\alpha}S(t) &= \Lambda+\phi R-\left(\frac{(1-ae)(\beta_a lA+\beta_s I)}{N}+\mu\right)S\\
{}_{0}^{ABC}D_t^{\alpha}E(t) &= \frac{(1-ae)(\beta_a lA+\beta_s I)}{N}-(\eta+\mu)E\\
{}_{0}^{ABC}D_t^{\alpha}A(t) &= (1-\theta)\eta E-(\rho+\mu+\upsilon)A\\
{}_{0}^{ABC}D_t^{\alpha}I(t) &= \theta\eta E-(\delta+\mu+\varepsilon+\tau)I\\
{}_{0}^{ABC}D_t^{\alpha}Q(t) &= \upsilon A+\tau I-(\omega+\mu)Q\\
{}_{0}^{ABC}D_t^{\alpha}R(t) &= \omega Q+\varepsilon I+\rho A-(\phi+\mu)R
\end{aligned}\right\} \tag{1}$$

3. Preliminary

Definition 1: **(Atangana and Baleanu, 2016, Caputo and Fabrizio, 2016)** The Mittage-Leffler function of one and two parameters denoted as $E_\alpha(z)$ and $E_{\alpha,\beta}(z)$, which is defined respectively as $E_\alpha(z)=\sum_{k=0}^{\infty}\frac{z^k}{\Gamma(\alpha k+1)}$ and $E_{\alpha,\beta}(z)=\sum_{k=0}^{\infty}\frac{z^k}{\Gamma(\alpha k+\beta)}$, $(\alpha>0,\quad \beta>0)$ where $z\in C$ and $\alpha,\beta\in C$

Definition 2: (Atangana *et al.*, 2020) The fractional integral associated with the new fractional derivative with non-local kernel is defined as

$${}_{a}^{AB}I_t^{\alpha}\left[\Omega(t)\right]=\frac{1-\alpha}{H(\alpha)}\Omega(t)+\frac{\alpha}{H(\alpha)\Gamma(\alpha)}\int_0^t\Omega(\xi)(t-\xi)^{\alpha-1}\,d\xi\,. \tag{2}$$

Definition 3: **(Atangana and Baleanu, 2016).** Let $\Omega\in C(a,b)$, $a<b$, $\alpha\in[0,1]$, then

$$ {}_{a}^{AB}I_t^{\alpha}\left[{}_{0}^{ABC}D_t^{\alpha}\Omega(t)\right]=\Omega(t)-\Omega(a). \tag{3}$$

Lemma 1: (Hossein and Moshen, 2018) Let $f(t)\in\mathbb{R}^{+}$ be a continuous and differentiable function. Then for any time instant $t\geq 0$

$$ {}_{0}^{ABC}D_t^{\alpha}\left(\Omega(t)-\Omega^{*}-\Omega^{*}\ln\frac{f(t)}{\Omega^{*}}\right)\leq\left(1-\frac{\Omega(t)}{\Omega^{*}}\right){}_{0}^{ABC}D_t^{\alpha}f(t). \tag{4}$$

4. Basic Properties of the Model

Theorem 1: Suppose that the initial data for the covid-19 model (1) be $S(0)>0,\ E(0)\geq 0,\ \mathrm{A}(0)\geq 0,\ I(0)\geq 0,\ Q(0)\geq 0,\ R(0)\geq 0,$, then the solution $S(t),\ E(t),\ A(t),\ I(t),\ Q(t)$ and $R(t)$ of the model with positive initial data will remain positive for all $t\geq 0$.

Proof

From the first equation of the covid-19 model (1), we have

$$ {}_{0}^{ABC}D_t^{\alpha}S(t)\geq-\left(\frac{(1-ae)(\beta_a lA+\beta_s I)}{N}+\mu\right)S \tag{5}$$

Following the approach in Atangana, (2023), and using definition 1, yields

$$\left.\begin{aligned}
S(t)&\geq S(0)E_{\alpha}\left(\frac{-t^{\alpha}\alpha\left(\beta_a l(1-ae)\|A\|_{\infty}+\beta_s(1-ae)\|I\|_{\infty}+\mu\right)}{\mathrm{H}(\alpha)+(1-\alpha)\left(\beta_a l(1-ae)\|A\|_{\infty}+\beta_s(1-ae)\|I\|_{\infty}+\mu\right)}\right),\quad \forall t\geq 0.\\
E(t)&\geq E(0)E_{\alpha}\left(\frac{-t^{\alpha}\alpha(\mu+\eta)}{\mathrm{H}(\alpha)+(1-\alpha)(\mu+\eta)}\right),\quad \forall t\geq 0\\
A(t)&\geq A(0)E_{\alpha}\left(\frac{-t^{\alpha}\alpha(\rho+\mu+\upsilon)}{\mathrm{H}(\alpha)+(1-\alpha)(\rho+\mu+\upsilon)}\right),\quad \forall t\geq 0\\
I(t)&\geq I(0)E_{\alpha}\left(\frac{-t^{\alpha}\alpha(\delta+\mu+\varepsilon+\tau)}{\mathrm{H}(\alpha)+(1-\alpha)(\delta+\mu+\varepsilon+\tau)}\right),\quad \forall t\geq 0\\
Q(t)&\geq Q(0)E_{\alpha}\left(\frac{-t^{\alpha}\alpha(\omega+\mu)}{\mathrm{H}(\alpha)+(1-\alpha)(\omega+\mu)}\right),\quad \forall t\geq 0\\
R(t)&\geq R(0)E_{\alpha}\left(\frac{-t^{\alpha}\alpha(\phi+\mu)}{\mathrm{H}(\alpha)+(1-\alpha)(\phi+\mu)}\right),\quad \forall t\geq 0
\end{aligned}\right\} \tag{6}$$

Hence all the solutions of the covid-19 model (1) remain positive for all $t\geq 0$.

Lemma 2: The closed set

$$\Delta=\left\{(S,E,A,I,Q,R)\in\mathbb{R}_{+}^{6};\ N\leq\frac{\Lambda}{\mu}\right\}$$

is positively- invariant and attract all the positive solutions of the model .

Proof

Adding equations in system (1), we have

$$ {}_{0}^{ABC}D_t^{\alpha} N \leq \Lambda - \mu N \quad (7)$$

Taking the Laplace transform of (7) and further simplification yield

$$N \leq \frac{\pi}{\mu}\left(1 - E_{\alpha}\left(-t^{\alpha}\frac{\alpha\mu}{\Phi}\right)\right) + \frac{1}{\Phi}E_{\alpha}\left(-t^{\alpha}\frac{\alpha\mu}{\Phi}\right)\left[\pi(1-\alpha) + H(\alpha)N(0)\right]$$

Since $E_{\alpha}\left(-\frac{\alpha\mu}{\Phi}t^{\alpha}\right)$, tends to zero monotonically as $t \to \infty$ (Choi *et al.,* 2014). In particular $N \leq \frac{\Lambda}{\mu}$. Hence, Δ is positively invariant and an attractor so that no solution path leaves through any boundary of Δ, where $\Phi = H(\alpha) + \mu(1-\alpha)$.

4. Local and global stability of the disease-free equilibrium

The disease-free equilibrium point ($\mathcal{E}_0$), is obtained as

$$\mathcal{E}_0 = \left\{\frac{\Lambda}{\mu}, 0, 0, 0, 0, 0\right\}$$

By utilizing the next generation matrix approach (Van den Driessche and Watmough, 2002) and using the symbols $\mathcal{F}$ and v, yield

$$\mathcal{F} = \begin{pmatrix} 0 & \beta_a l(1-ae) & \beta_s(1-ae) \\ 0 & 0 & 0 \\ 0 & 0 & 0 \end{pmatrix} \text{ and } v = \begin{pmatrix} h_1 & 0 & 0 \\ -(1-\theta)\eta & h_2 & 0 \\ -\theta\eta & 0 & h_3 \end{pmatrix}$$

Consequently, the basic number for reproduction ($\mathcal{R}_0$) is provided as

$$\mathcal{R}_0 = \rho\left(\mathcal{F}v^{-1}\right) = \mathcal{R}_1 + \mathcal{R}_2$$

where, $\mathcal{R}_1 = \dfrac{\beta_a l(1-ae)(1-\theta)\eta}{(\mu+\eta)(\mu+\upsilon+\rho)}$ and $\mathcal{R}_2 = \dfrac{\beta_a l(1-ae)\theta\eta}{(\mu+\eta)(\mu+\varepsilon+\tau+\delta)}$

$h_1 = \mu + \eta$, $h_2 = \mu + \upsilon + \rho$, $h_3 = \mu + \varepsilon + \tau + \delta$, $h_4 = \mu + \omega$, $h_5 = \mu + \phi$.

Lemma 3: The COVID-19 system (1) exhibits a locally asymptotically stable disease-free equilibrium $\mathcal{E}_0$, when $\mathcal{R}_0 < 1$ and an unstable equilibrium whenever $\mathcal{R}_0 > 1$

Proof

The COVID-19 system's Jacobian matrix is provided by

$$J(\mathcal{E}_0) = \begin{bmatrix} -\mu & 0 & -\beta_a(1-ae)l & -\beta_s(1-ae) & 0 & \phi \\ 0 & -h_1 & \beta_a(1-ae)l & \beta_s(1-ae) & 0 & 0 \\ 0 & (1-\theta)\eta & -h_2 & 0 & 0 & 0 \\ 0 & \theta\eta & 0 & -h_3 & 0 & 0 \\ 0 & 0 & \upsilon & \tau & -h_4 & 0 \\ 0 & 0 & \rho & \varepsilon & \omega & -h_5 \end{bmatrix}$$

Clearly we observed that $-\mu,\ -h_4$ and $-h_5$ are eigenvalues of the matrix, the remaining are obtained from the polynomial

$$P(\chi)=\chi^3+b_2\chi^2+b_1\chi+b_0=0 \tag{9}$$

where

$b_2=h_2+h_3+h_4,\ \ b_1=h_1h_2\left(1-\mathcal{R}_1\right)+h_1h_3\left(1-\mathcal{R}_2\right)+h_2h_3,\ \ b_0=h_1h_2h_3\left(1-\mathcal{R}_0\right)$

Now, applying the Routh-Hurwitz criterion (Hassan *et al.,* 2022) which implies that the eigenvalues of (9) are all negative if and only if $b_i>0,\ i=1,2,3, b_2>0,\ b_0>0$ and $b_2b_1>b_0$ and $\mathcal{R}_0<1.$ Hence, $\chi_i<0\ \ (i=1,2,\dots,6), \arg(\chi_i)=\pi\ \ \arg(\chi_i)=\pi\geq\alpha\dfrac{\pi}{2}$, which implies that $\mathcal{E}_0$, is locally asymptotically stable.

Theorem 2: The COVID-19 model disease-free equilibrium. $\mathcal{E}_0$ is globally asymptotically stable within the feasible interval if $\mathcal{R}_0<1$ and unstable if $\mathcal{R}_0>1$:

Proof.

Using the Lyapunov function denoted by

$$\mathcal{L}=\mathcal{R}_0E+\frac{\beta_a l(1-ae)}{h_2}A+\frac{\beta_s(1-ae)}{h_3}I \tag{10}$$

whose fractional derivative is

$${}_{0}^{ABC}D_t^{\alpha}\mathcal{L}=\mathcal{R}_0\left(\frac{(1-ae)(\beta_a lA+\beta_s I)S}{N}-h_1E\right)+\frac{\beta_a l(1-ae)}{h_2}\left((1-\theta)\eta E-h_2A\right)+\frac{\beta_s(1-ae)}{h_3}(\theta\eta E-h_3I)$$

yields,

$${}_{0}^{ABC}D_t^{\alpha}\mathcal{L}=\beta_a l(1-ae)A\left(\frac{\mathcal{R}_0S}{N}-1\right)+\beta_s(1-ae)I\left(\frac{\mathcal{R}_0S}{N}-1\right)$$

$${}_{0}^{ABC}D_t^{\alpha}\mathcal{L}\leq\beta_a l(1-ae)A(\mathcal{R}_0-1)+\beta_s(1-ae)I(\mathcal{R}_0-1)$$

$${}_{0}^{ABC}D_t^{\alpha}\mathcal{L}\leq(1-ae)(\beta_a lA+\beta_s I)(\mathcal{R}_0-1)$$

Hence ${}_{0}^{ABC}D_t^{\alpha}\mathcal{L}\leq 0$ if and only if $\mathcal{R}_0<1$ and ${}_{0}^{ABC}D_t^{\alpha}\mathcal{L}=0$ if and only if $A=I=0$. Since all the parameters are non-negative it follows that, $\mathcal{L}$ is a Lyapunov function on Δ. Furthermore the largest compact invariant set in $\left\{\left(S^*(t),E^*(t),A^*(t),I^*(t),Q^*(t),R^*(t)\right)\in\Delta:\ {}_{0}^{ABC}D_t^{\alpha}\mathcal{L}=0\right\}$ is the singleton set ($\mathcal{E}_0$). Therefore by LaSalle's Invariant Principles (LaSalle, 1968) every solution to the model with initial condition in Δ, approaches $\mathcal{E}_0$ as $t\to\infty$ whenever $\mathcal{R}_0<1$ so that $\mathcal{E}_0$ is GAS in Δ if $\mathcal{R}_0<1$.

5. Global Stability Endemic Equilibrium Point ($\mathcal{E}_1$)

Let $\mathcal{E}_1=\left\{S^{**},E^{**},A^{**},I^{**},Q^{**},R^{**}\right\}$ be the endemic equilibrium point. It is obtained by setting the RHS of the system (1) to zero. Hence, the positive endemic equilibrium point is obtained when $\mathcal{R}_0>1$, as

$$S^{**}=\frac{\Lambda h_1h_2h_3h_4h_5}{h_1h_2h_3h_4h_5\left(\mu+Z_1\right)+ZZ_1\theta}\qquad E^{**}=\frac{\Lambda h_2h_3h_4h_5Z_1}{h_1h_2h_3h_4h_5\left(\mu+Z_1\right)+ZZ_1\theta}$$

$$A^{**}=\frac{\Lambda(1-\theta)\eta h_3h_4h_5Z_1}{h_1h_2h_3h_4h_5(\mu+Z_1)+ZZ_1\theta}\qquad I^{**}=\frac{\Lambda\theta\eta h_3h_4h_5Z_1}{h_1h_2h_3h_4h_5(\mu+Z_1)+ZZ_1\theta}$$

$$Q^{**}=\frac{\Lambda Z_1h_5\left(\eta\theta\upsilon h_1+\eta(1-\theta)\tau h_2\right)}{h_1h_2h_3h_4h_5(\mu+Z_1)+ZZ_1\theta}\qquad R^{**}=\frac{\Lambda ZZ_1}{h_1h_2h_3h_4h_5(\mu+Z_1)+ZZ_1\theta}$$

$$Z=\omega\left(\eta\theta\upsilon h+\eta(1-\theta)\tau h_2\right)+\eta(1-\theta)\rho h_1h_4+\varepsilon(1-\theta)\rho h_2h_4$$

$$Z_1=\frac{\Lambda h_1h_2h_3h_4h_5(\mathcal{R}_0-1)}{\Lambda h_1h_2h_3h_4h_5+\Lambda\theta\eta h_3h_4h_5+\Lambda(1-\theta)\eta h_3h_4h_5+\Lambda h_5\left(\eta\theta\upsilon h_1+\eta(1-\theta)\tau h_2\right)+\Lambda Z}$$

Theorem 4: The COVID-19 model endemic equilibrium, $\mathcal{E}_1$ is globally asymptotically stable within the feasible interval if $\mathcal{R}_0>1$

Proof

Consider the function

$$\mathcal{M}=\left(S-S^{**}-S\ln\frac{S^{**}}{S}\right)+\left(E-E^{**}-E^{**}\ln\frac{E^{**}}{E}\right)+\frac{\beta_a lA^{**}S^{**}}{\theta\eta E^{**}}\left(A-A^{**}-A^{**}\ln\frac{A^{**}}{A}\right)$$
$$+\frac{\beta_s I^{**}S^{**}}{(1-\theta)\eta E^{**}}\left(I-I^{**}-I^{**}\ln\frac{I^{**}}{I}\right)$$

whose fractional derivative

$${}_0^{ABC}D_t^{\alpha}\mathcal{M}={}_0^{ABC}D_t^{\alpha}\left(S-S^{**}-S\ln\frac{S^{**}}{S}\right)+{}_0^{ABC}D_t^{\alpha}\left(E-E^{**}-E^{**}\ln\frac{E^{**}}{E}\right)$$
$$+\left(\frac{\beta_a lA^{**}S^{**}}{\theta\eta E^{**}}\right){}_0^{ABC}D_t^{\alpha}\left(A-A^{**}-A^{**}\ln\frac{A^{**}}{A}\right)+\left(\frac{\beta_s I^{**}S^{**}}{(1-\theta)\eta E^{**}}\right){}_0^{ABC}D_t^{\alpha}\left(I-I^{**}-I^{**}\ln\frac{I^{**}}{I}\right)$$

Using lemma 1, yield

$${}_0^{ABC}D_t^{\alpha}\mathcal{M}\le\left(1-\frac{S^{**}}{S}\right){}_0^{ABC}D_t^{\alpha}S+\left(1-\frac{E^{**}}{E}\right){}_0^{ABC}D_t^{\alpha}E+\frac{\beta_a lA^{**}S^{**}}{\theta\eta E^{**}}\left(1-\frac{A^{**}}{A}\right){}_0^{ABC}D_t^{\alpha}A$$
$$+\frac{\beta_s I^{**}S^{**}}{(1-\theta)\eta E^{**}}\left(1-\frac{I^{**}}{I}\right){}_0^{ABC}D_t^{\alpha}I$$

$${}_0^{ABC}D_t^{\alpha}\mathcal{M}\le\left(1-\frac{S^{**}}{S}\right)\left(\Lambda+\phi R-\left((1-ae)(\beta_a lA+\beta_s I)+\mu\right)S\right)$$
$$+\left(1-\frac{E^{**}}{E}\right)\left(\left((1-ae)(\beta_a lA+\beta_s I)+\mu\right)S-h_1E\right)$$
$$+\frac{\beta_a lA^{**}S^{**}}{\theta\eta E^{**}}\left(1-\frac{A^{**}}{A}\right)\left((1-\theta)\eta E-h_2A\right)+\frac{\beta_s I^{**}S^{**}}{(1-\theta)\eta E^{**}}\left(1-\frac{I^{**}}{I}\right)(\theta\eta E-h_3I)$$

Further simplification

$$
{}^{ABC}_{\;\;0}D_t^{\alpha}\mathcal{M} \le \mu S^{**}\left(2-\frac{S}{S^{**}}-\frac{S^{**}}{S}\right)+\beta_a lA^{**}S^{**}\left(3-\frac{S^{**}}{S}-\frac{ASE^{**}}{A^{**}S^{**}E}-\frac{EA^{**}}{AE^{**}}\right)\sqrt{b^2-4ac}
$$
$$
+\beta_s I^{**}S^{**}\left(3-\frac{S^{**}}{S}-\frac{ISE^{**}}{I^{**}S^{**}E}-\frac{EI^{**}}{IE^{**}}\right)+\theta R\left(\frac{R^{**}}{R}-1\right)\left(\frac{S^{**}}{S}-1\right)
$$

Since the arithmetic mean exceeds the geometric mean the following inequalities hold;

$$
2-\frac{S}{S^{**}}-\frac{S^{**}}{S}\le 0,\quad 3-\frac{S^{**}}{S}-\frac{ASE^{**}}{A^{**}S^{**}E}-\frac{EA^{**}}{AE^{**}}\le 0,\; 3-\frac{S^{**}}{S}-\frac{ISE^{**}}{I^{**}S^{**}E}-\frac{EI^{**}}{IE^{**}}\le 0,
$$

Furthermore, since all the model are non-negative, thus ${}^{ABC}_{\;\;0}D_t^{\alpha}\mathcal{M}\le 0$, if $S^{**}=S$, $A^{**}=A$, $E^{**}=E$, $I^{**}=I$, $R^{**}=R$ then the largest compact invariant set in Δ such that ${}^{ABC}_{\;\;0}D_t^{\alpha}\mathcal{M}\le 0$ is the singleton set ($\mathcal{E}_1$) then by LaSalle Invariant Principle (LaSalle, 1968) it implies $\mathcal{E}_1$, is globally asymptotically stable (GAS) in the interior of Δ.

6. Model Fitting

We fitted the covid-19 model (1) using daily data from the NCDC for the period of March 4, 2022, to April 30, 2022. Figure 4 shows the least square fit model's time series depiction. The developed model was fitted using nonlinear least squares method, which involved using the built-in Matlab R2023a and the optimizer function "*fminsearch*" to determine the values of the unknown parameter, υ and τ . The initial values of the stated variables are: $S(0)=20000$, $E(0)=50$, $A(0)=0$, $I(0)=1$, $Q(0)=0$ and $R(0)=0$.

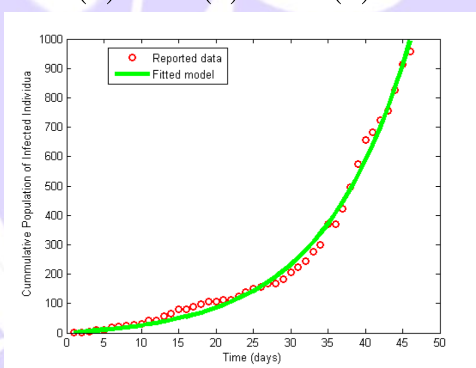

Figure 2: Comparison of the predicted (solid curve) and observed (dotted lines) covid-19 cumulative data from the CDC, Nigeria.

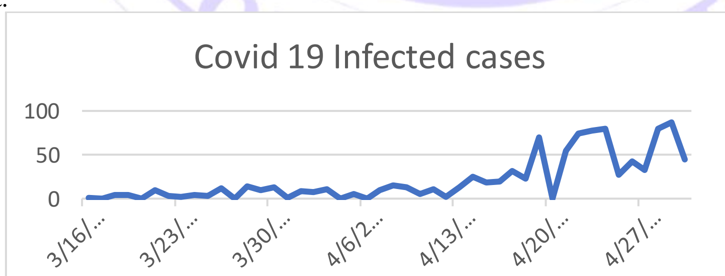

Figure 3: Number of infected people in Lagos, Nigeria from 16 March 2020 to 30th April, 2020

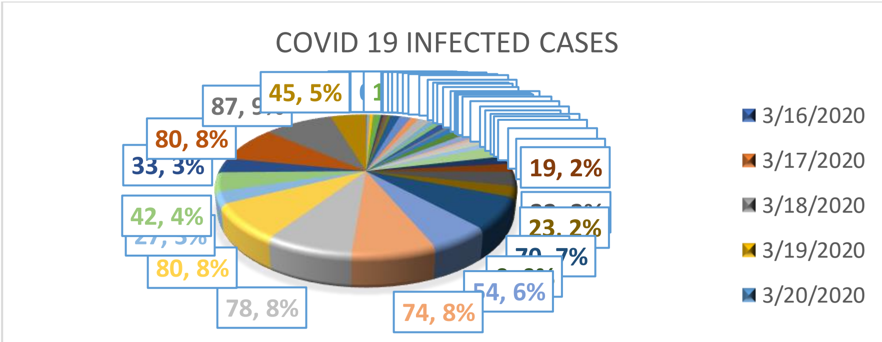

Figure 4: Number of infected people in Lagos, Nigeria from 16 March 2020 to 30th April, 2020

7. Sensitivity Analysis

Sensitivity analysis shows how important each parameter is for the transmission of illness. It is employed to determine which components, due to their substantial influence, require intervention efforts. Sensitivity indices allow us to evaluate the proportionate change in a variable that results from a change in a parameter. The normalized forward sensitivity index of a variable with regard to a parameter is the ratio of the relative change in the variable to the relative change in the parameter. The ratio of the relative change in the variable to the relative change in the parameter is the normalized forward sensitivity index of a variable with respect to a parameter. As can be seen in Table 1, every factor has a positive index. This means that if one parameter (β_a, β_s, l) is raised while the others stay the same, the effective reproduction number will rise as well, raising the likelihood of an epidemic. But, the parameters $(\rho, \upsilon, \delta, \mu, \eta, \varepsilon, a, e, \tau)$ indices are negative, which means that increasing one while maintaining the others lowers the effective reproduction number and, thus, the covid-19 load on human populations.

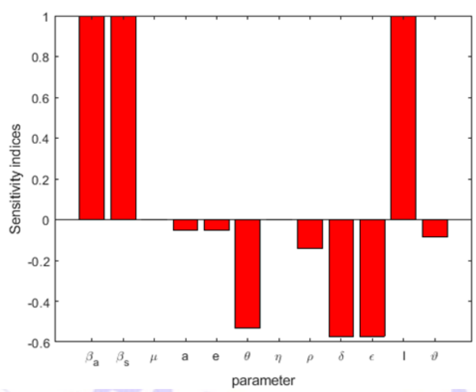

Figure 5: Sensitivity indices of the basic reproduction number in relation to the reproduction number's parameter values.

Table 1: Effect of parameter β_a and β_s on $\mathcal{R}_0$

S/N	β_a	β_s	$\mathcal{R}_0$
1	0.102	0.255	0.6342
2	0.302	0.455	1.1357
3	0.502	0.755	1.8845
4	0.702	0.855	2.1385
5	0.802	0.955	2.3892

Table 2: Effect of parameter a and e on $\mathcal{R}_0$

S/N	a	e	$\mathcal{R}_0$
1	0.100	0.100	2.2146
2	0.300	0.200	2.1028
3	0.600	0.400	1.7001
4	0.800	0.700	0.9843
5	0.900	0.900	0.4250

Table 3: Parameter Values

Parameter	Value	Sources
Λ	750/day	Abioye *et al.,* 2021
β_a	0.302/day	Iboi *et al.,* 2020
β_s	0.855/day	Iboi *et al.,* 2020
μ	0.0004/day	Muhammad *et al.,* 2020
δ	0.00286/day	Abioye *et al.,* 2021
υ	0.8533/day	Fitted
ε	1/7/day	Iboi *et al.,* 2020
ρ	1/7/day	Iboi *et al.,* 2020
τ	0.1038/day	Fitted
e	0.1/ dimensionless	Iboi *et al.,* 2020
a	0.5/ dimensionless	Iboi *et al.,* 2020
ω	0.0766/day	Abioye *et al.,* 2021
η	1/6/day	Iboi *et al.,* 2020
ϕ	0.00229/day	Abioye *et al.,* 2021
l	0.1	Fang *et al.,* 2022
θ	0.35/ dimensionless	Iboi *et al.,* 2020

8. Numeral Scheme and Simulation

Utilizing the methodology described by Toufit and Atangana (2017), we developed the numerical scheme for the COVID-19 model (1), which is provided as

$$
\begin{aligned}
S(t_{k+1}) &= S(t_0) + \frac{1-\alpha}{H(\alpha)}\Omega_1\left(t_k, S(t_k)\right) \\
&+ \frac{\alpha}{H(\alpha)\Gamma(\alpha)}\sum_{i=1}^{k}\left[\frac{\Omega_1\left(t_i, S(t_i)\right)}{\Gamma(\alpha+2)}h^{\alpha}\left[(k-i+2+\alpha)(k+1-i)^{\alpha}-(k-i+2+2i)(k-i)^{\alpha}\right]\right] \\
&- \frac{\alpha}{H(\alpha)\Gamma(\alpha)}\sum_{i=1}^{k}\left[-\frac{\Omega_1\left(t_{i-1}, S(t_{j-1})\right)}{\Gamma(\alpha+2)}h^{\alpha}\left[(k+1-i)^{\alpha+1}-(k-i+1+i)(k-i)^{\alpha}\right]\right]
\end{aligned}
$$

$$E\left(t_{k+1}\right)=E\left(t_0\right)+\frac{1-\alpha}{H(\alpha)}\Omega_2\left(t_k,E\left(t_k\right)\right)$$
$$+\frac{\alpha}{H(\alpha)\Gamma(\alpha)}\sum_{i=1}^{k}\left[\frac{\Omega_2\left(t_i,E\left(t_i\right)\right)}{\Gamma(\alpha+2)}h^{v}\left[(k-i+2+v)(k+1-i)^{\alpha}-(k-i+2+2i)(k-i)^{\alpha}\right]\right]$$
$$-\frac{\alpha}{H(\alpha)\Gamma(\alpha)}\sum_{i=1}^{k}\left[-\frac{\Omega_2\left(t_{i-1},E\left(t_{j-1}\right)\right)}{\Gamma(\alpha+2)}h^{\alpha}\left[(k+1-i)^{\alpha+1}-(k-i+1+i)(k-i)^{\alpha}\right]\right]$$

$$A\left(t_{k+1}\right)=A\left(t_0\right)+\frac{1-\alpha}{H(\alpha)}\Omega_3\left(t_k,A\left(t_k\right)\right)$$
$$+\frac{\alpha}{H(\alpha)\Gamma(\alpha)}\sum_{i=1}^{k}\left[\frac{\Omega_3\left(t_i,A\left(t_i\right)\right)}{\Gamma(\alpha+2)}h^{\alpha}\left[(k-i+2+\alpha)(k+1-i)^{\alpha}-(k-i+2+2i)(k-i)^{\alpha}\right]\right]$$
$$-\frac{\alpha}{H(\alpha)\Gamma(\alpha)}\sum_{i=1}^{k}\left[-\frac{\Omega_3\left(t_{i-1},A\left(t_{j-1}\right)\right)}{\Gamma(\alpha+2)}h^{\alpha}\left[(k+1-i)^{\alpha+1}-(k-i+1+i)(k-i)^{\alpha}\right]\right]$$

$$I\left(t_{k+1}\right)=I\left(t_0\right)+\frac{1-\alpha}{H(\alpha)}\Omega_4\left(t_k,I\left(t_k\right)\right)$$
$$+\frac{\alpha}{H(\alpha)\Gamma(\alpha)}\sum_{i=1}^{k}\left[\frac{\Omega_4\left(t_i,I\left(t_i\right)\right)}{\Gamma(\alpha+2)}h^{\alpha}\left[(k-i+2+\alpha)(k+1-i)^{\alpha}-(k-i+2+2i)(k-i)^{\alpha}\right]\right]$$
$$-\frac{\alpha}{H(\alpha)\Gamma(\alpha)}\sum_{i=1}^{k}\left[-\frac{\Omega_4\left(t_{i-1},I\left(t_{j-1}\right)\right)}{\Gamma(\alpha+2)}h^{\alpha}\left[(k+1-i)^{\alpha+1}-(k-i+1+i)(k-i)^{\alpha}\right]\right]$$

$$Q\left(t_{k+1}\right)=Q\left(t_0\right)+\frac{1-\alpha}{H(\alpha)}\Omega_5\left(t_k,Q\left(t_k\right)\right)$$
$$+\frac{\alpha}{H(\alpha)\Gamma(\alpha)}\sum_{i=1}^{k}\left[\frac{\Omega_5\left(t_i,Q\left(t_i\right)\right)}{\Gamma(\alpha+2)}h^{\alpha}\left[(k-i+2+\alpha)(k+1-i)^{\alpha}-(k-i+2+2i)(k-i)^{\alpha}\right]\right]$$
$$-\frac{\alpha}{H(\alpha)\Gamma(\alpha)}\sum_{i=1}^{k}\left[-\frac{\Omega_5\left(t_{i-1},Q\left(t_{j-1}\right)\right)}{\Gamma(\alpha+2)}h^{\alpha}\left[(k+1-i)^{\alpha+1}-(k-i+1+i)(k-i)^{\alpha}\right]\right]$$

$$
\begin{aligned}
R\left(t_{k+1}\right) &= R\left(t_0\right) + \frac{1-\alpha}{H(\alpha)}\Omega_6\left(t_k, R\left(t_k\right)\right) \\
&+ \frac{\alpha}{H(\alpha)\Gamma(\alpha)}\sum_{i=1}^{k}\left[\frac{\Omega_6\left(t_i, R\left(t_i\right)\right)}{\Gamma(\alpha+2)}h^{\alpha}\left[\left(k-i+2+\alpha\right)\left(k+1-i\right)^{\alpha} - \left(k-i+2+2i\right)\left(k-i\right)^{\alpha}\right]\right] \\
&- \frac{\alpha}{H(\alpha)\Gamma(\alpha)}\sum_{i=1}^{k}\left[-\frac{\Omega_6\left(t_{i-1}, R\left(t_{j-1}\right)\right)}{\Gamma(\alpha+2)}h^{\alpha}\left[\left(k+1-i\right)^{\alpha+1} - \left(k-i+1+i\right)\left(k-i\right)^{\alpha}\right]\right]
\end{aligned}
$$

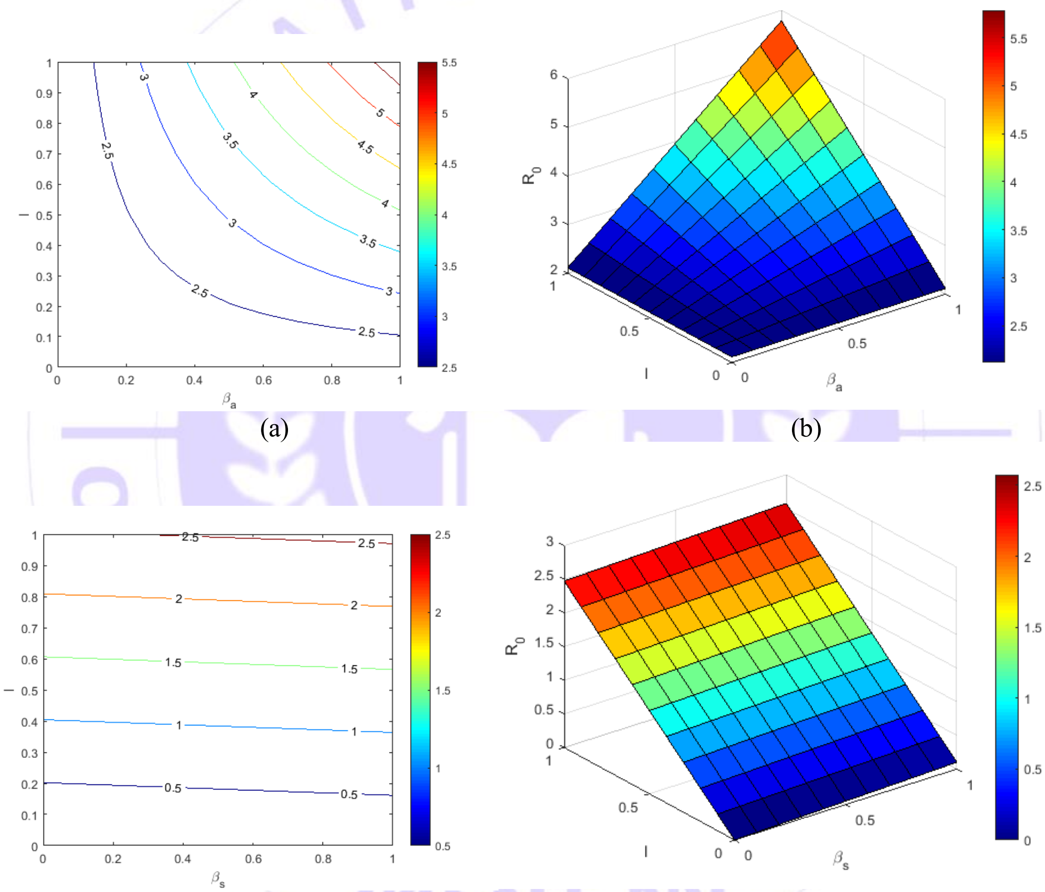

(a) (b)

(c) (d)

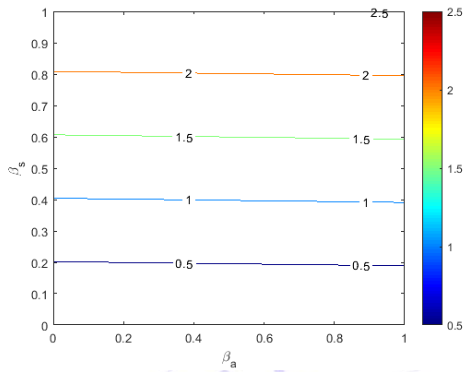

(e)

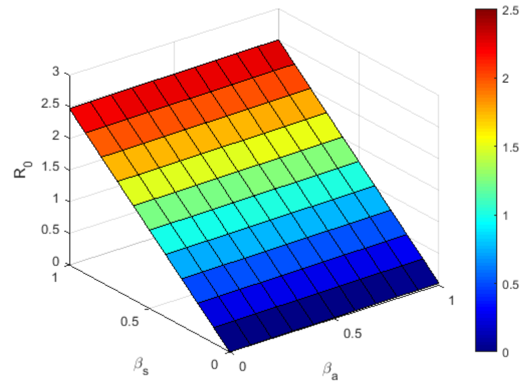

(f)

Figure 6: Basic reproduction number contour plots as a function (a) l vs β_a (b) l vs β_s (c) β_a vs β_s.

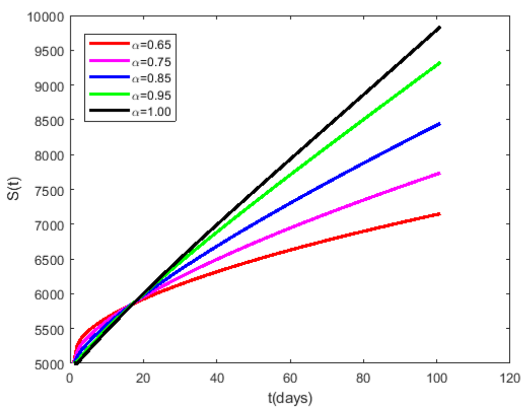

(a)

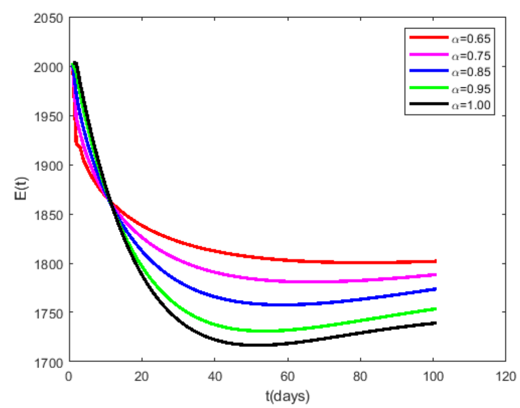

(b)

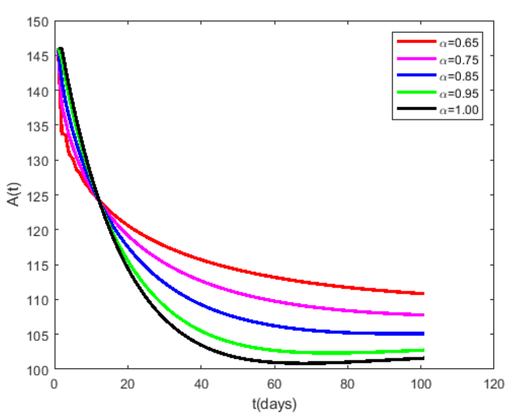

(c)

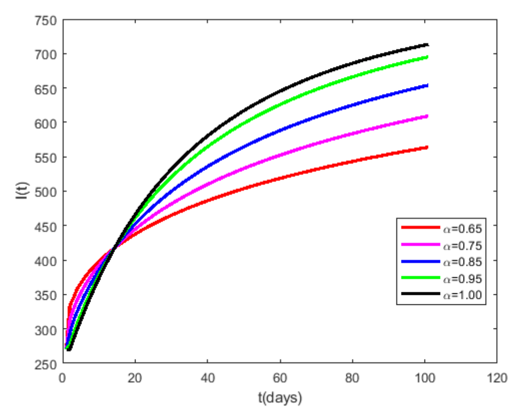

(d)

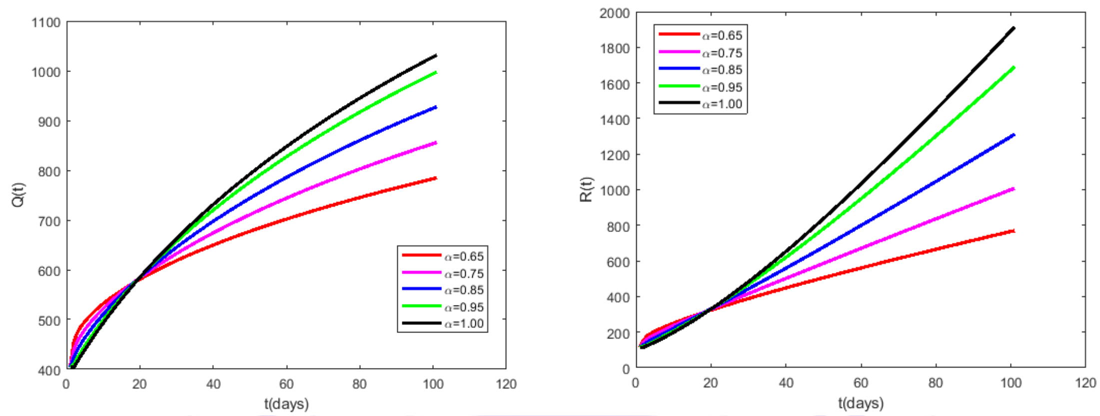

(e) (f)

Figure 7: COVID-19 model (1) numerical visualization with various fractional orders:

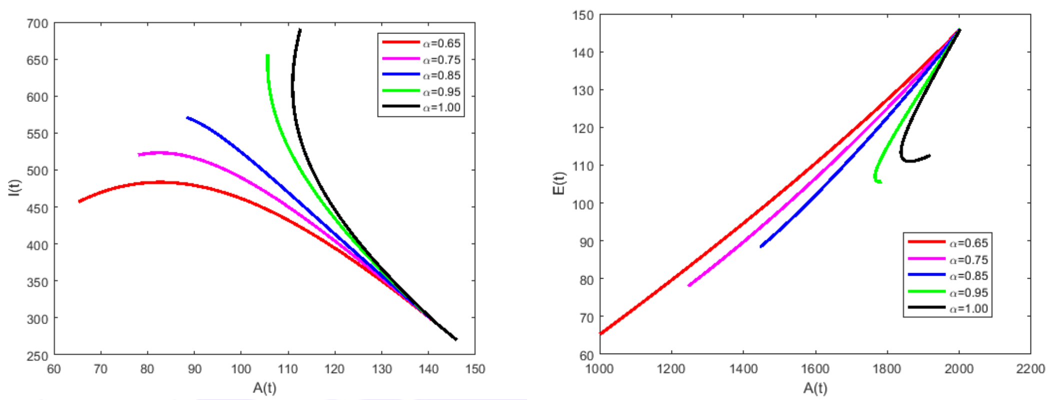

(a) (b)

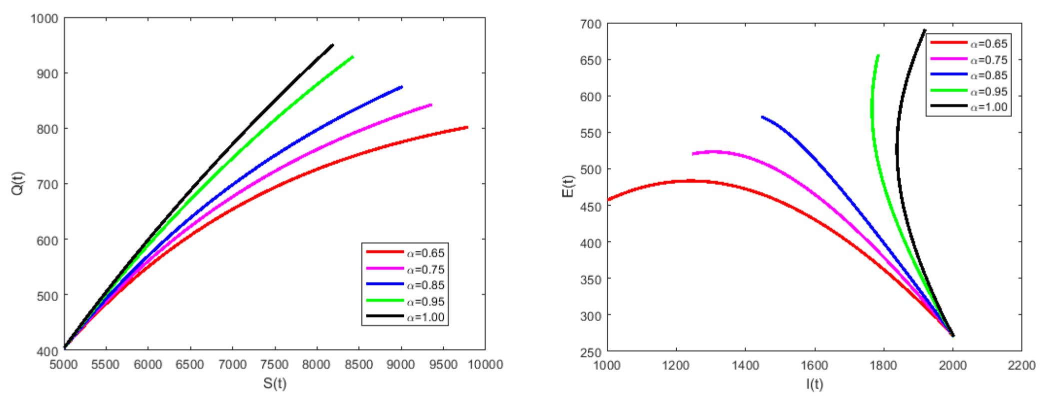

(c) (d)

Figure 8: A numerical simulation demonstrating the COVID-19 model's phase portrait with varying fractional orders:

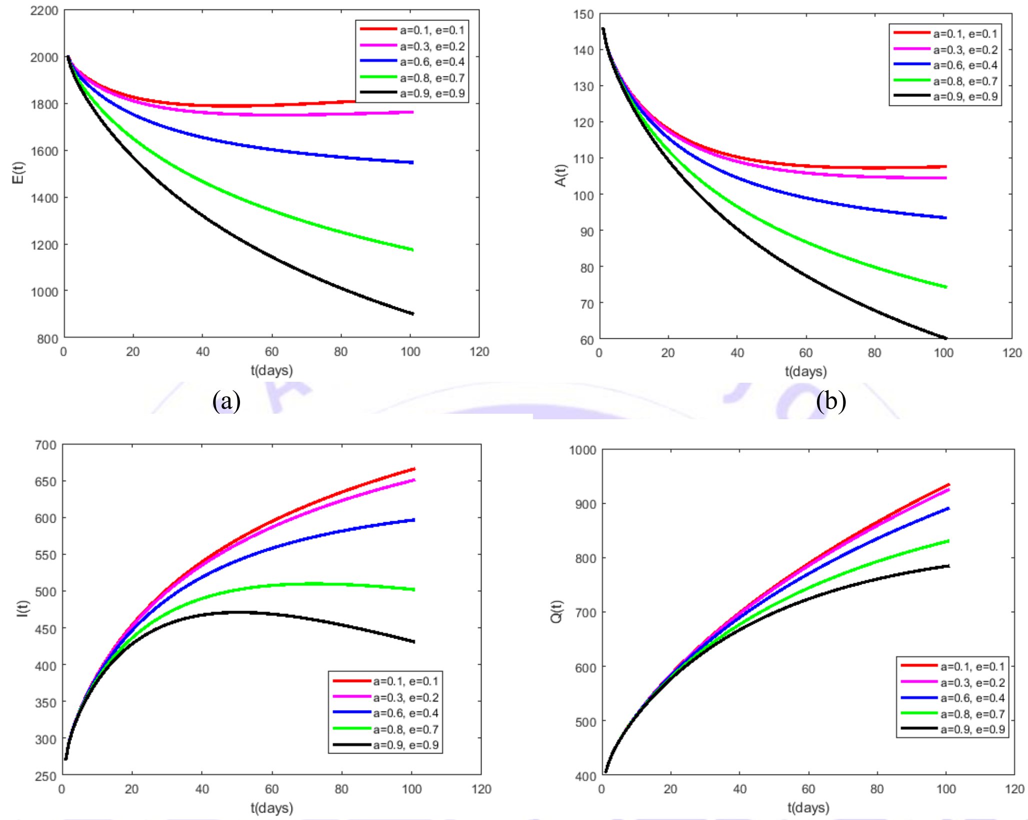

(a) (b)

(c) (d)

Figure 9: A numerical simulation demonstrating the effect of a face mask on $E(t)$, $A(t)$, $I(t)$ and $Q(t)$, for order $\alpha = 0.85$.

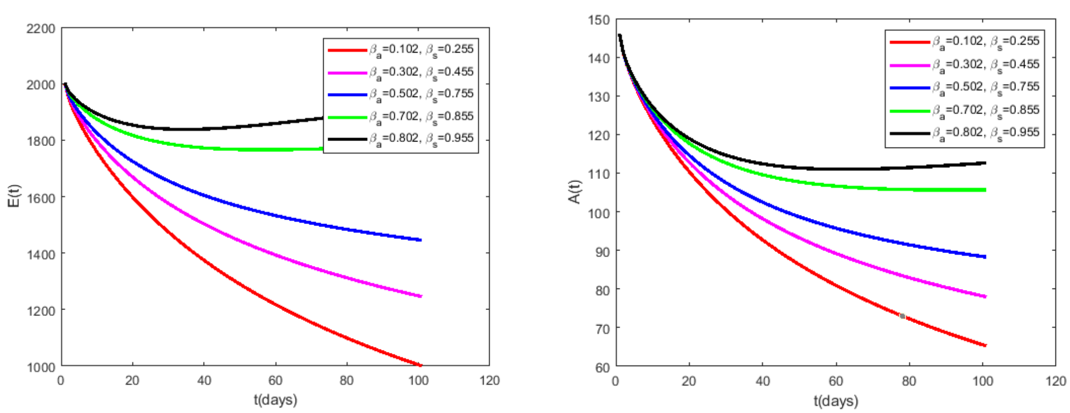

(a) (b)

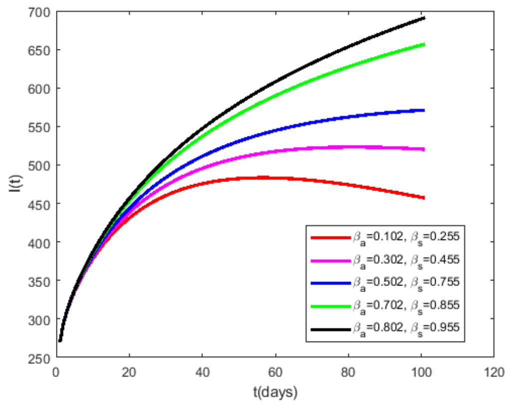

(c)

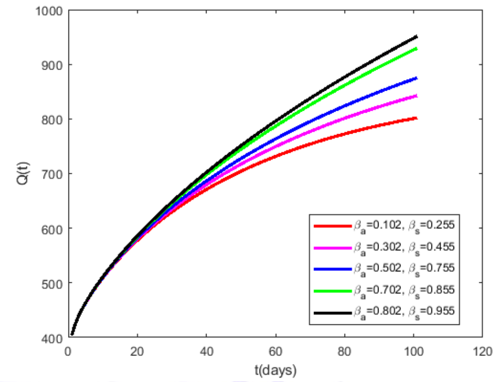

(d)

Figure 10: A numerical simulation illustrating the influence of the contact rates $(\beta_a \text{ and } \beta_s)$, on $E(t),\ A(t),\ I(t)$ and $Q(t)$, for order $\alpha = 0.85$.

The behavior of susceptible population $S(t)$, exposed population $E(t)$, asymptomatic population $A(t)$ symptomatic population $I(t)$ quarantine population $Q(t)$ and recovered population $R(t)$ was plotted against time t in days for both fractional and integer transmissions, with $\alpha = 0.65,\ 0.75,\ 0.85,\ 0.95$ and $\alpha = 1$ for the latter. Figure 7(a) shows an increase in people who are susceptible, which suggests a decline in immunity or an increase in susceptibility as a result of factors like waning immunity, a decline in the use of preventative measures, or the appearance of novel variations. A greater number of individuals displaying COVID-19 symptoms and increased rates of infection and transmission are shown by the rise in the symptomatic population seen in Figure 7(d). A decrease in the quantity of people exposed to the virus, as seen in Figure 7(b), indicates a shorter incubation period or lower rates of transmission, thereby exposing fewer people to the virus. The reduction in the quantity of asymptomatic cases can be attributed to several factors, such as enhanced detection and identification of asymptomatic cases, decreased likelihood of asymptomatic infection, or modifications in the pathogenicity of the virus, as illustrated in figure 7(c). An increase in the number of individuals under quarantine is seen in Figure 7(e), which is in line with increased efforts to stop the infection from spreading by isolating infected individuals from those who have had intimate contact with confirmed cases. The growing number of recovered individuals is depicted in Figure 7(f), which may be related to the disease's natural progression or efficacious treatment. The contour plot of the fundamental reproduction number, $(\mathcal{R}_0)$ as a function of the transmissibility rate of the asymptomatic class against the contact rate is displayed in Figure 6(a-d). Transmissibility causes $\mathcal{R}_0$ to increase, indicating that the illness has the potential to spread. A higher likelihood of an epidemic outbreak is indicated by a rise in both transmissibility rates and contact rate of the asymptomatic individuals. An increase in $\mathcal{R}_0$ indicates higher transmissibility and potential for persistent transmission, when both the effective rate of the asymptomatic class and the effective contact rate of the symptomatic class increase. Important insights into the long-term dynamics of the disease within a community can be gained from the plot of endemic equilibria (Figure 8(a-d)) of the COVID model (1), which shows effective preventative strategies or reducing new infections. The basic reproduction number, $\mathcal{R}_0$ of less than 1 indicates a decline in cases, indicating stability. However, a $\mathcal{R}_0$ value greater than 1 suggests exponential growth, potentially leading to outbreaks and difficulties in controlling the disease's spread. In the case of $a = 0.1$ and $e = 0.1$ (poor compliance and mask effectiveness) $\mathcal{R}_0 = 2.2146$. This scenario implies that the virus can propagate significantly with low compliance and mask efficacy, resulting in a reasonably high $\mathcal{R}_0$. It suggests that variables other than mask use are mostly responsible for the virus's propagation. At $a = 0.3$ and $e = 0.2$ (moderate compliance and moderate mask efficacy), $\mathcal{R}_0 = 2.1028$: Here, the fraction of people wearing masks and their effectiveness both have a moderate influence on lowering transmission. The fact that $\mathcal{R}_0$ has not decreased significantly, nevertheless, suggests that more steps might be required to further restrict the spread. When $a = 0.6$ and $e = 0.4$ (moderate compliance and strong mask efficacy) $\mathcal{R}_0 = 1.7001$. In this case, a sizable section of the populace is using masks, which have a comparatively high effectiveness. This result in a significant drop in $\mathcal{R}_0$, indicating that mask use is essential for controlling the virus's spread. When $a = 0.8$ and $e = 0.7$ (very high effectiveness of masks and high compliance) $\mathcal{R}_0 = 0.9843$:- Here, both the effectiveness of masks and the compliance rate are high. Consequently, $\mathcal{R}_0$ drops below 1, indicating that each infected individual, on average, infects less than one other person. This suggests that the spread of the covid-19 virus is under control, and the epidemic is likely to decline. When $a = 0.9$ and $e = 0.9$ (very high mask effectiveness and nearly universal compliance) $\mathcal{R}_0 = 0.4250$. The virus spread is greatly suppressed in this ideal situation, where masks are very effective and almost everyone wears them. $\mathcal{R}_0$ is well below 1, indicating that the epidemic is likely to end quickly as shown in Table 2 and Figure 10(a-d). When both asymptomatic and symptomatic persons have low effective contact rates, $\beta_a = 0.102$ and $\beta_s = 0.255$, respectively, $\mathcal{R}_0 = 0.6342$ is obtained. In this case, the effective contact rates of both symptomatic and asymptomatic persons are rather low. This results in a low $\mathcal{R}_0$, which suggests that the virus's spread is successfully under control. This is probably because fewer people of both categories are transmitting the infection. $\mathcal{R}_0 = 1.1357$ is reached when $\beta_a = 0.302$ and $\beta_s = 0.455$ (moderate effective contact rates): Both symptomatic and asymptomatic subjects have modest effective contact rates in this case. As a consequence, the $\mathcal{R}_0$ is moderate, indicating that although the virus can spread, control efforts might still be successful in keeping the epidemic under control. $\mathcal{R}_0 = 1.8545$, when $\beta_a = 0.502$ and $\beta_s = 0.755$ (high effective contact rates) are present. Both sick and asymptomatic persons have high effective contact rates in this setting. As a result $\mathcal{R}_0$ rises, suggesting a greater chance of viral dissemination. Control strategies become increasingly difficult, and actions might be required to lessen the spread of the disease. $\mathcal{R}_0 = 2.1385$, when $\beta_a = 0.702$ and $\beta_s = 0.855$ (very high effective contact rates). Both asymptomatic and symptomatic subjects have extremely high rates of successful contact in this case. This leads to a noticeably increased $\mathcal{R}_0$, indicating that the infection is spreading quickly. Robust control mechanisms are required to stop cases from growing exponentially. $\mathcal{R}_0 = 2.3892$ shows, both asymptomatic and symptomatic persons have very high effective contact rates when $\beta_a = 0.802$ and $\beta_s = 0.955$ (very high effective contact rates). $\mathcal{R}_0$ is therefore much higher, suggesting a significant probability of broad transmission as shown in Table 1 and Figure 9(a-d). To stop a serious outbreak, intensive control measures are necessary. The plot offers important insights into the mechanisms of disease and informs public health initiatives.

9. Conclusion

A covid-19 model using the ABC operator was designed and used to study disease transmission dynamics. The basic reproduction number obtained indicates stability in the system, with a value below 1, indicating stability, and a value above 1 indicating exponential growth, potentially causing outbreaks and uncontrollable disease control. The plot of endemic equilibria in a covid-19 model provides insights into the long-term dynamics of the disease within a population. The model's simulation demonstrated that the plot depicts the dissemination of covid-19 and reveals varying degrees of efficacy and compliance. While low compliance and mask efficacy lead to virus propagation, high compliance and mask effectiveness contribute to lower transmission. Effective masks and high compliance are essential for control. Successful control is indicated by low effective contact rates, or social distance; high rates raise the danger of viral spread. Public health initiatives are informed by this information.

Reference

Adel, W., Günerhan, H., Nisar, K. S., Agarwal, P., & El-Mesady, A. (2024). Designing a novel fractional order mathematical model for COVID-19 incorporating lockdown measures. *Scientific Reports*, *14*(1). https://doi.org/10.1038/s41598-023-50889-5.

Ahmed, I., Baba, I. A., Yusuf, A., Kumam, P., & Kumam, W. (2020). Analysis of Caputo fractional-order model for COVID-19 with lockdown. *Advances in Difference Equations*, *2020*(1). https://doi.org/10.1186/s13662-020-02853-0.

Abioye A. I., Peter, O. J., Ogunseye, H. A., Oguntolu, F. A., Oshinubi, K., Ibrahim, A. A. & Khan, I. (2021). Mathematical model of COVID-19 in Nigeria with optimal control. *Results in Physics*, *28*, 104598. https://doi.org/10.1016/j.rinp.2021.104598

Alam, M.T., Sohail, S.S., Ubaid, S., Ali, Z., Hijji, M., Saudagar, A.K.J. & Muhammad, K. (2022). It's your turn, are you ready to get vaccinated? Towards an exploration of vaccine hesitancy using sentiment analysis of Instagram posts. *Mathematics*, 10, 4165.

Akinyemi A. I & Isiugo-Abanihe U. C. (2014). Demographic dynamics and development in nigeria. African Population Studies. 27:239–48.

Atangana, A. (2021). Mathematical model of survival of fractional calculus, critics and their impact: How singular is our world?. *Adv Differ Equ*. 403 (2021). https://doi.org/10.1186/s13662-021-03494-7.

Atangana A. & Baleanu D. (2016). New fractional derivatives with nonlocal and non-singular kernel theory and application to heat transfer model, *Therm. Sci.*, **20**, 763–769.

Baba, I. A., Ahmed, I., Al-Mdallal, Q. M., Jarad, F., & Yunusa, S. (2022). Numerical and theoretical analysis of an awareness COVID-19 epidemic model via generalized Atangana-Baleanu fractional derivative. *Journal of Applied Mathematics and Computational Mechanics*, *21*(1), 7–18. https://doi.org/10.17512/jamcm.2022.1.01.

Brauer, F. (2005). The Kermack-McKendrick epidemic model revisited. *Math. Biosci*. 2005, 198, 119–131.

Caputo M. & Fabrizio M. (2015). A new definition of fractional derivatives without singular kernel, *Prog. Fract. Differ. Appl.*, **1**. 1–13.

Castilho, C., Gondim, J.A.M., Marchesin, M. & Sabeti, M. (2020). Assessing the efficiency of different control strategies for the COVID-19 epidemic. Electron. *J. Differ. Equ*. 64, 1–17.

Choi, S. K., Kang, B. & Koo, N. (2014). Stability for Caputo Fractional Differential Systems. *Abstract and Applied Analysis*, *2014*, 1–6. https://doi.org/10.1155/2014/631419.

Cortés-Carvajal, P.D., Cubilla-Montilla, M. & González-Cortés, D.R. (2022). Estimation of the instantaneous reproduction number and its confidence interval for modeling the COVID-19 pandemic. *Mathematics*. 10, 287.

Ega, T. T. & Ngeleja, R. C. (2022). Mathematical Model Formulation and Analysis for COVID-19 Transmission with Virus Transfer Media and Quarantine on Arrival. *Computational and Mathematical Methods*, *2022*, 1–16. https://doi.org/10.1155/2022/2955885

Ferguson, N., Laydon, D., Nedjati Gilani, G., Imai, N., Ainslie, K., Baguelin, M. & Perez, Z.C. (2020). *Impact of Non-Pharmaceutical Interventions (NPIs) to Reduce COVID-19 Mortality and Healthcare Demand*; Imperial College London: London, UK.

Hassan, T. S., Elabbasy, E. M., Matouk, A., Ramadan, R. A., Abdulrahman, A. T. & Odi- naev I. (2022). RouthHurwitz Stability and Quasiperiodic Attractors in a Fractional-Order Model for Awareness Programs: Applications to COVID-19 Pandemic. *Discrete Dynamics in Na- ture and Society*; 115. https://doi.org/10.1155/2022/1939260

Hossein, K. & Mohsen, J. (2018). Optimal control of a fractional-order model for the HIV/AIDS epidemic. *Int. J. Biomath*. 11(7):1850086.

Hou, C., Chen, J., Zhou, Y., Hua, L., Yuan, J., He, S., Guo, Y., Zhang, S., Jia, Q., Zhao, C. *et al*. (2020). The effectiveness of quarantine of Wuhan city against the corona virus disease 2019 (COVID-19): A well-mixed SEIR model analysis. *J. Med. Virol.* 92, 841–848.

Iboi E. A., Ngonghala, C. N. & Gumel, A. B. (2020). Will an imperfect vaccine curtail the COVID-19 pandemic in the U.S.? *Infectious Disease Modelling*, *5*, 510–524. https://doi.org/10.1016/j.idm.2020.07.006.

Jia, J., Ding, J., Liu, S., Liao, G., Li, J., Duan, B., Wang, G. & Zhang, R. (2020). Modeling the control of COVID-19: Impact of policy interventions and meteorological factors. Electron. *J. Differ. Equ*. 23, 1–24.

Kim Y., Lee S., Chu C., Choe S., Hong S. & Shin Y. (2016). The characteristics of Middle Eastern respiratory syndrome coronavirus transmission dynamics in South Korea. Osong *Public Health Res Perspectives*. 7(1):49–55.

LaSalle, J. P. Stability theory for ordinary equations. *J Differ Equ*. 4(1968): 57-65.

Madubueze C., E, Kimbir A., R & Aboiyar T. (2018). Global Stability of Ebola Virus Disease Model with Contact Tracing and Quarantine. *Appl Appl Math*.13 (1):382–403.

NCDC, (2020). Nigeria Center for Disease Control. [Online]. Available: http://covid19. ncdc.gov.ng/. Accessed 7 September 2020.

Nguyen, P.H., Tsai, J.F., Lin, M.H. & Hu, Y.C. (2021). A hybrid model with spherical fuzzy-AHP, PLS-SEM and ANN to predict vaccination intention against COVID-19. *Mathematics* 2021, 9, 3075.

Okyere, S., Ackora-Prah, J., Abdullah, S., Adarkwa, S. A., Owusu, F. K., Bonsu, K., Fokuo, M. O., & Yeboah, M. A. (2023). Analysis of Turberculosis-COVID-19 Coinfection Using Fractional Derivatives. *International Journal of Mathematics and Mathematical Sciences*, *2023*, 1–14. https://doi.org/10.1155/2023/2831846

Peng, L., Yang, W., Zhang, D., Zhuge, C. & Hong, L. (2020). Epidemic analysis of COVID-19 in China by dynamical modeling. arXiv:2002.06563.

Podlubny, I. (1999). Fractional differential equations, 198 academic press. San Diego, California, USA.

Prem, K., Liu, Y., Russell, T.W., Kucharski, A.J., Eggo, R.M., Davies, N. & Klepac, P. (2020). The effect of control strategies to reduce social mixing on outcomes of the COVID-19 epidemic in Wuhan, China: A modelling study. *Lancet Public Health*. 5, e261–e270.

Saleem, S., Rafiq, M., Ahmed, N., Arif, M. S., Raza, A., Iqbal, Z., Niazai, S., & Khan, I. (2024, April 8). Fractional epidemic model of coronavirus disease with vaccination and crowding effects. *Scientific Reports*, *14*(1). https://doi.org/10.1038/s41598-024-58192-7

Shaikh, A. S., Shaikh, I. N., & Nisar, K. S. (2020). A mathematical model of COVID-19 using fractional derivative: outbreak in India with dynamics of transmission and control. *Advances in Difference Equations*, *2020*(1). https://doi.org/10.1186/s13662-020-02834-3

Sinan, M., & Alharthi, N. H. (2023). Mathematical Analysis of Fractal-Fractional Mathematical Model of COVID-19. *Fractal and Fractional*, *7*(5), 358. https://doi.org/10.3390/fractalfract7050358.

Sun, T. C., DarAssi, M. H., Alfwzan, W. F., Khan, M. A., Alqahtani, A. S., Alshahrani, S. S. & Muhammad, T. (2023). Mathematical Modeling of COVID-19 with Vaccination Using Fractional Derivative: A Case Study. *Fractal and Fractional*, *7*(3), 234. https://doi.org/10.3390/fractalfract7030234

Toufik, M. & Atangana, A. (2017). New numerical approximation of fractional derivative with non- local and non-singular kernel: Application to chaotic models. *The European Physical Journal Plus.* 132(10). https://doi.org/10.1140/epjp/i2017-11717-0
technical-guidance.

Vasily, E. T. (2018) Generalized Memory: fractional calculus approach. *Fractal fract*. 2(4):23.

Van den Driessche, P. & Watmough, P. (2002). *Reproduction numbers and sub-threshold endemic equilibria for compartmental models of disease transmission*. *Math. Biosci*, 180: 29–48.

Worldometers. COVID-19 Coronavirus Pandemic. 2021. Available online: https://www.worldometers.info/coronavirus/(accessed on 8 July 2023).

World Health Organization, (2020). Coronavirus Disease (COVID-19) Technical Guidance. Available from: https://www.who.int/emergencies/diseases/novel-coronavirus-2019/

Xu J. & Tang Y. (2021) Bayesian framework for multi-wave COVID-19 epidemic analysis using empirical vaccination data. *Mathematics*, 10, 21.